2005 American Control Conference
June 8-10, 2005. Portland, OR, USA

Slip controller design and implementation in a Continuously Variable Transmission

R. J. Pulles, B. Bonsen, M. Steinbuch and P. A. Veenhuizen

Abstract— **Continuously Variable Transmissions (CVT) can be used to operate a combustion engine in a more optimal working point. Unfortunately, due to the relatively low efficiency of modern production CVT's the total efficiency of the driveline is not increased significantly. This low efficiency is mainly caused by losses in the hydraulic actuation system and the variator. Decreasing the clamping forces in the variator greatly improves the efficiency of the CVT. However, lower clamping forces increase the risk of excessive belt slip, which can damage the system. In this paper a method is presented to measure and control slip in a CVT in order to minimize the clamping forces while preventing destructive belt slip. To ensure robustness of the system against torque peaks, a controller is designed with optimal load disturbance response. A synthesis method for robust PI(D)-controller design is used to maximize the integral gain while making sure that the closed loop system remains stable. Experimental results prove the validity of the approach.**

I. Introduction

Fuel consumption and driveline efficiency are important issues in the automotive industry. Continuously Variable Transmissions (CVT) can cover a wide range of ratio's, which makes it possible to operate a combustion engine in more efficient working points than stepped transmissions. This decreases the fuel consumption of the engine, but because of the relatively low efficiency of a CVT compared to manual transmissions the total driveline efficiency is not increased significantly.

The main reason for the low efficiency of modern production CVT's are the high clamping forces in the variator necessary to prevent belt slip. Heavy belt slip can cause severe damage to the belt and pulleys of the variator, resulting in lower performance of the CVT in time. To prevent belt slip at all times, the clamping forces in modern production CVT's are usually much higher (typically 30% or more) than needed for normal operation. Higher clamping forces result in additional losses in both the hydraulic and the mechanical system. This is due to increased pump losses and friction losses because of the extra mechanical load that is applied on all parts, particularly on the variator.

Studies have shown that reducing the clamping forces in a CVT result in a remarkable increase in efficiency [1], [2]. However, it also increases the risk of excessive belt slip when torque peaks act on the driveline. But belt slip does not always lead to damage to the belt and pulleys, as recent research shows [3]. No damage occurs as long as certain limits in belt slip speed and belt normal forces are not exceeded. In this paper, a method is presented to measure and control slip in a modern production CVT, namely the Jatco CK2 [4]. By using slip control it is possible to operate the CVT with minimal clamping forces, resulting in a higher efficiency, while preventing excessive belt slip. The most important requirement of the slip controller is that it has the ability to attenuate the load disturbances caused by torque peaks in the driveline. An additional problem in the controller design process is that the slip dynamics change for different values of ratio and speed. Therefore a robust gain-scheduled controller is desirable. To meet all requirements, a synthesis method for robust PI(D)-controllers with optimal load disturbance response is used [5]. The designed slip controller is simulated and subsequently tested on a test rig that is equipped with a 2.0-liter Internal Combustion Engine (ICE), a flywheel, an eddy-current brake, and a disc brake to simulate realistic road loads.

II. Continuously Variable Transmission

A. Working principle

In this research program the Jatco CK2 is used for testing, which is based on the metal push belt from Van Doorne's Transmissie (VDT). Fig. 1 shows the layout of the variator, which is the key element of a CVT. The variator consists of a V-shaped metal belt between two sets of conical sheaves, also called pulleys. Both pulley sets have a fixed and a moveable pulley, opposed to each other. The movable pulleys are actuated by hydraulic pressure cylinders. By adjusting the position of the pulleys the ratio of the variator is changed. The variator can cover any ratio between the two extremes shown in Fig. 1, low and overdrive (OD).

R. J. Pulles, B. Bonsen, M. Steinbuch and P. A. Veenhuizen are with the Eindhoven University of Technology, Department of Mechanical Engineering, Den Dolech 2, 5600 MB, Eindhoven
phone: +31 40 247 48 17; fax:+31 40 246 14 18;
email:b.bonsen@tue.nl

0-7803-9098-9/05/$25.00 ©2005 AACC

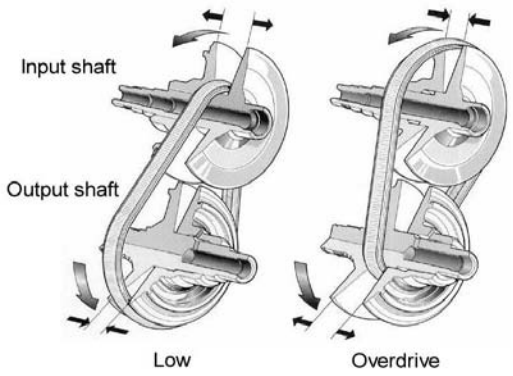

Fig. 1. Working principle of a Continuously Variable Transmission

The speed ratio of the variator is defined as:

$$r_s = \frac{\omega_s}{\omega_p} \quad (1)$$

Where ω_s represents the angular speed of the secondary (output) shaft and ω_p the angular speed of the primary (input) shaft.

Power is transmitted by means of friction between the belt and the pulleys. The torque that is transmitted through the variator can be calculated using the force balance on a pulley, according to [2]:

$$T_{cvt,p,s} = \frac{2\min(F_s, F_p)R_{p,s}\mu}{\cos\alpha} \quad (2)$$

Where $T_{cvt,p,s}$ is the transmitted torque for respectively the primary and the secondary shaft, $F_{p,s}$ is the primary or secondary clamping force, which is the force applied by the respective pulleys onto the belt, $R_{p,s}$ represent the primary and secondary running radius of the belt respectively, α is the pulley wedge angle and μ is the traction coefficient between belt and pulley. The traction coefficient μ is not constant but depends on the relative slip between the belt and the pulleys, defined as [2]:

$$v = 1 - \frac{r_s}{r_{s0}} \quad (3)$$

Where r_{s0} is defined as the speed ratio when no torque is applied to the secondary variator shaft. The ratio r_{s0} can be reconstructed by measuring the position of one of the moveable pulleys using a linear displacement sensor. First the output of the displacement sensor is measured under no-load conditions for all ratios. The relationship between r_{s0} and the output of the displacement sensor is approximated using a sixth order polynomial, which is then used to reconstruct the no-load ratio r_{s0}.

The relation between the traction coefficient μ and the slip v is shown in Fig. 2 [6]. It can be seen that the slope of the curves and the maximum traction coefficients clearly depend on the ratio, but all curves show the same distinct shape. At first, for low slip values the traction coefficient increases with increasing slip, until a maximum value is reached. This region is called the microslip region. When the maximum value of the traction coefficient is reached, increasing slip will result in a slow decrease of the traction coefficient. This region is known as the macroslip region.

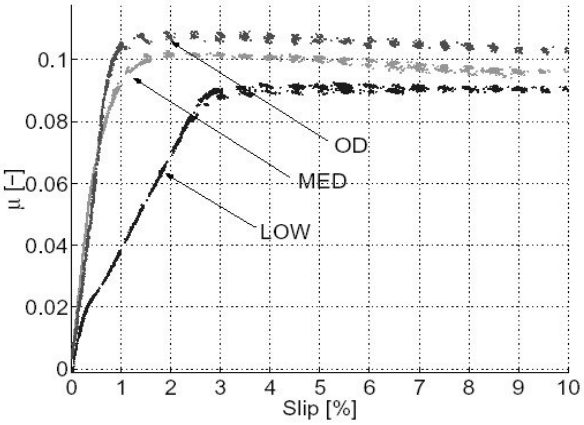

Fig. 2. Traction coefficient μ as a function of the relative slip measured with an input speed of 300 rad/s for ratios low (0.43), medium (1) and overdrive (2.25)

B. Clamping force strategies

An increase in torque in the variator will lead to more slip. When the slip level remains in the microslip region, an increase in slip will also lead to an increasing traction coefficient, thus allowing the higher torque to be transmitted. In the macroslip region however, slip will increase drastically if no action is taken when the torque increases.

The majority of the current clamping force strategies are designed to keep the slip values within the microslip region at all times to prevent belt damage. This is achieved by applying a clamping force that is high enough to transmit the engine torque that is based on an estimation from the Engine Control Module (ECM). To make sure that torque shocks will not trigger excessive slip, this clamping force is multiplied by a safety factor of at least 1.3. Additionally a safety margin on the clamping force is added for low engine torques. Since the engine torque is in general relatively low in normal operation, the clamping forces are much too high most of the time. This contributes greatly to the low efficiency of modern CVT's mentioned earlier.

Using slip control, the clamping forces are actively controlled to maximize the efficiency of the CVT. This is achieved by maintaining an amount of slip, where the traction coefficient is near its maximum [2]. This means that the slip is controlled in the transition area of the micro- and macroslip regions. An increase in the torque level will lead to an increase in belt slip, but by adjusting the clamping force fast enough the slip will not reach destructive levels and therefore damage can be avoided.

III. SLIP DYNAMICS

A. Modeling slip dynamics

To be able to design a slip controller, the slip dynamics are modelled. The model is based on the CVT dynamics presented in Fig. 3, where T_e and J_e represent the engine torque and inertia respectively, T_d and J_d represent the driveline torque and inertia and $T_{cvt,p,s}$ are given by (2).

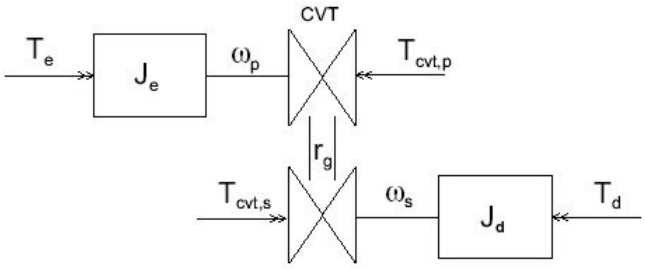

Fig. 3. CVT dynamics

The relative slip v is based on the no-load ratio r_{s0}, which is experimentally obtained as mentioned earlier. Since this is not very suitable for modeling purposes, the geometric ratio r_g is used instead, which is a good approximation of r_{s0}, defined as:

$$r_g = \frac{R_p}{R_s} \tag{4}$$

In this model the geometric ratio is assumed quasi-stationary. This is possible because the geometric ratio has much slower dynamics than the slip dynamics during normal operation of a CVT. Based on this assumption, the slip dynamics can be derived using (1) and (3), resulting in:

$$\dot{\nu} = -\frac{\dot{r}_s}{r_g} \tag{5}$$

$$\dot{r}_s = \frac{\dot{\omega}_s \omega_p - \omega_s \dot{\omega}_p}{\omega_p^2} \tag{6}$$

With r_g quasi-stationary, the dynamics of the CVT can be described by:

$$\dot{\omega}_p = \frac{T_e - T_{cvt,p}}{J_e} \tag{7}$$

$$\dot{\omega}_s = \frac{T_{cvt,s} - T_d}{J_d} \tag{8}$$

Combining (1)-(8) results in the following expression for the slip dynamics:

$$\dot{\nu} = \frac{1}{\omega_p}\left(-\frac{2FR_s\mu(\nu)}{\cos(\alpha)J_d r_g} + \frac{T_d}{J_d r_g}\right) + \frac{(1-\nu)}{\omega_p}\left(-\frac{2FR_s r_g \mu(\nu)}{\cos(\alpha)J_e} + \frac{T_e}{J_e}\right). \tag{9}$$

The derived dynamics for the slip are nonlinear. For controller design purposes, the system will be linearized around different operating points. With the linearized model a state space representation of the system will be defined.

For this purpose the traction coefficient is taken piecewise linear, to describe the micro- and macroslip region. Indicating the different regions with index i, the traction coefficient can be written as:

$$\mu = k_{1,i}\nu + k_{2,i} \tag{11}$$

Defining the state space as $x = \nu$, and $u = \begin{bmatrix} F & T_e & T_d \end{bmatrix}^T$ the system can be linearized around a certain working point $x = \nu_0$, resulting in the linear system:

$$\dot{\hat{x}} = A\hat{x} + B\hat{u} \tag{12}$$

Where $\hat{x} = x - x_0$ and $\hat{u} = u - u_0$. The linearized matrices A and B can now be derived:

$$A = \frac{1}{\omega_{p0}}\left[-\frac{T_{e0}}{J_e} - \rho_0\psi_0 F_0 k_{1i} + \frac{\rho_0 F_0 r_{g0} k_{2i}}{J_e}\right] \tag{13}$$

$$B = \frac{1}{\omega_{p0}}\begin{bmatrix} -\rho_0\psi_0 k_{2i} - \rho_0\psi_0\nu_0 k_{1i} + \dfrac{\rho_0 r_{g0}\nu_0 k_{2i}}{J_e} \\ \dfrac{(1-\nu_0)}{J_e} \\ \dfrac{1}{J_d r_{g0}} \end{bmatrix}^T \tag{14}$$

Where $\rho_0 = \dfrac{2R_{s0}}{\cos(\alpha)}$ and $\psi_0 = \left(\dfrac{r_{g0}}{J_e} + \dfrac{1}{J_d r_{g0}}\right)$ are introduced for writing convenience. Using (2) T_{e0} in (13) is calculated from the other values to match the maximum torque that can be transmitted in the chosen working point, this results in:

$$T_{e0} = \rho_0 F_0 r_{g0} \mu(\nu_0) \tag{15}$$

The linearization process of (9) also produces a higher order term in both A and B, but these are neglected because they are more than one order smaller than the other terms.

The derived linearized system will be used for controller design. This model has 3 inputs, but only the clamping force F_s can be controlled on implementation. The input torque T_e is controlled by the driver via the throttle pedal and the output torque T_d is determined by road conditions. Therefore they can be regarded as disturbances acting on the system.

B. FRF-measurements actuation system

The clamping force in the Jatco CK2 is applied using hydraulic pressure cylinders attached to the movable pulleys [4]. The oil pressure in the cylinders is regulated by a complex electro-hydraulic actuation system that is controlled by a PWM-based solenoid. The duty cycle of the PWM-signal determines the oil pressure that provides the clamping force, or the line pressure. The line pressure in the CK2 is limited between 0.66 and 4.2 MPa, between these values the pressure varies practically linear with the

duty cycle. Modeling this electro-hydraulic system is a complex and time-consuming task. Therefore the system's dynamic response is determined using FRF-measurements. A good estimation of the system's response will then be used in the controller design process.

For the FRF-measurements, the duty cycle of the solenoid is taken as the input and the line pressure as the output. The measurements were performed at different pressures, ratios, and engine speeds. All measurements showed practically identical system responses, only with slightly different gains for low frequencies, but small enough to be neglected. Fig. 4 shows the result of one of the FRF-measurements.

The system is estimated with a third order low-pass filter with a cut-off frequency of 6 Hz, which is also plotted in the figure. The frequency of the PWM signal is 50 Hz, this causes a peak in the FRF. Because the bandwidth of the system is much lower than 50 Hz it is not taken into account in the estimation.

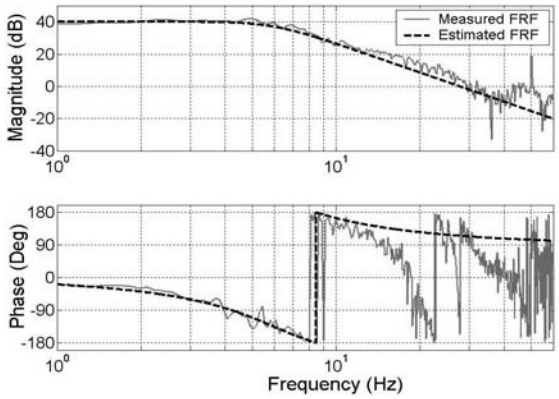

Fig. 4. Measured and estimated FRF of the line pressure circuit in the Jatco CK2

IV. SLIP CONTROLLER DESIGN

A. The control design problem

With the linearized model of the slip dynamics and the estimated transfer function of the actuation system a slip controller can be designed. The slip dynamics are highly nonlinear and depend on many variables. Using (13) and (14) the variables that influence the slip dynamics the most can be found. There is a great difference in the system response between the micro- and macroslip region. For slip control design, attention is mainly focused on the macroslip region. In this region, ratio and primary speed have the largest influence on the dynamics. Because the dynamics depend on so many variables, it is practically impossible to design a controller that is stable in all situations and still has the desired performance.

To tackle this problem a gain-scheduled linear controller will be designed. This is done by linearizing the slip dynamics in a number of working points and calculate the controller parameters for each working point. As mentioned earlier, the slip controller requires good load disturbance attenuation and must be robust to deal with model uncertainties. For this purpose a gain-scheduling PID-controller was proposed. However, due to the large amount of measurement noise in automotive applications the derivative term cannot be used. Therefore a gain-scheduling PI-controller is proposed, as shown in Fig. 5. As can be seen, the gain is scheduled based on primary speed, ratio, and slip. Slip is used to determine whether the system is in the micro- or macroslip region. The setpoint also varies with the ratio, since the maximum traction coefficient is reached for different slip values, depending on the ratio. This is shown in Fig. 2.

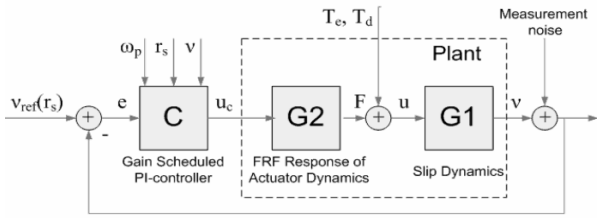

Fig. 5. Proposed slip controller

B. Robust PI-controller synthesis method

To easily design controller parameters for multiple working points, while meeting both design requirements, a synthesis method for robust PI(D)-controllers with optimal load disturbance response is used [5]. The method is based on a constrained optimization problem that maximizes the integral gain of the PI(D)-controller while making sure that the maximum sensitivity is less than a specified value. Using the maximum sensitivity as the main design parameter, a trade-off can be made between load disturbance response and robustness with respect to model uncertainties.

The resulting controller parameters of this optimization process can be obtained graphically for a PI-controller. It produces a series of ellipses in the controller parameter space, called the *k-ki* plane, for different frequencies of the system. These ellipses represent a boundary for the sensitivity constraint, and together they form a boundary surface in the *k-ki* plane. Choosing combinations of *k* and *ki* below this surface ensures a stable and robust closed loop system. For optimal load disturbance attenuation, the maximum value of the integral gain is determined from the figure. The proportional gain is then determined graphically. Fig. 6 shows a typical result of the synthesis method.

Using this synthesis method for different ratios in the micro- and macroslip region, the gain-scheduling scheme presented in Table I is obtained. The differences between the micro- and macroslip region mentioned earlier, result in very different values for the controller parameters. This is

because the system dynamics drastically change at the transition from the micro- to the macroslip region. The system matrix A in (12) almost becomes zero in the macroslip region. This means that a part of the system dynamics disappear, resulting in great changes in the system's gain.

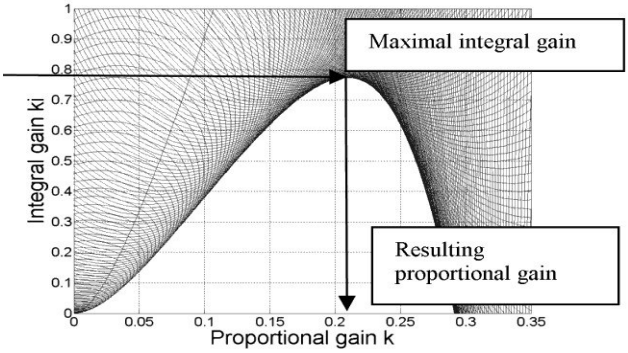

Fig. 6. Example of the sensitivity constraint in k-ki plane

Another reason is that in the macroslip region the system's gain becomes scalable by the primary speed ω_p. This can be seen in (14), considering the fact that system matrix A is practically zero. Therefore the gains in Table I for the macroslip region are scaled by the primary speed (in rad/s) in the controller.

TABLE I
CONTROLLER PARAMETERS FOR VARIOUS WORKING POINTS

	Microslip region		Macroslip region	
Ratio	P-gain	I-gain	P-gain (@ 100 rad/s)	I-gain (@ 100 rad/s)
0.43	1.7	30	0.435	1.61
1	1.9	53	0.294	1.087
2.25	3.6	110	0.21	0.772

Based on ratio, slip, and primary speed, the proper controller parameters are used. Between the working points shown in table I interpolation will be used. To ensure the stability of the controller between these working points, several measures were taken. In the microslip region load disturbance response is not very important since slip will not cause any damage in this region. However, many model uncertainties are present, because the slip dynamics depend on many variables in this region. Therefore a maximum sensitivity of 1.2 is chosen in the controller synthesis method, which is relatively low. In the macroslip region a maximum sensitivity of 1.8 is chosen, this is much higher since there are less model uncertainties in this region and good load disturbance response is required.

C. Controller implementation

In order to successfully implement the controller described in the previous section, an integral anti-windup is added. This is necessary because the output of the controller is limited between the minimum and maximum pressure level of the CK2. To prevent slip caused by the engine torque T_e a feed forward term is added based on (2), which calculates the minimal clamping force to transmit the given engine torque. The engine torque is estimated using the engine speed and the throttle valve position. This feed forward is needed because the bandwidth of the slip controller is not sufficient to compensate for the fast dynamics of a combustion engine. With these additions the slip controller is ready for implementation.

V. RESULTS

A. Test Setup

The developed slip controller will be implemented on a test rig. Fig. 7 shows a schematic representation of the test rig. It is designed to perform realistic drive train experiments, using a combustion engine as the power source and a flywheel, an eddy-current brake, and a disc brake to simulate road loads. The torques on the input and output shaft of the transmission are measured using telemetry systems. The Jatco CK2 can be controlled with the Transmission Control Module (TCM) that is used in a car or with the newly developed slip controller. This is very useful for efficiency comparison.

Slip is not measured directly, but is calculated from other signals, based on (3). The angular speeds of the primary and secondary shaft of the CVT are measured to determine the ratio r_s. The no-load ratio r_{s0} is determined using a LVDT to measure the displacement of the primary pulley, as described earlier. The system is accurate enough to detect 0.1% slip, which should be sufficient to implement the slip controller.

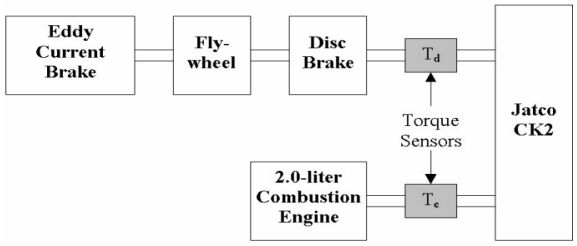

Fig. 7. Test rig used for experiments

B. Efficiency measurements

Slip control is developed to improve the efficiency of CVT's, therefore efficiency measurements are carried out to proof what the benefits of the slip controller are in a production CVT. The efficiency when using the TCM is compared to the efficiency when using the slip controller. The efficiency comparison is carried out at fixed ratios and with a constant engine speed of 300 rad/s. The slip value is controlled between 0.5% for ratio 2.25 (overdrive) and 1.5% for ratio 0.43 (low). At these slip values the maximum efficiency of the CK2 is reached. The engine torque is gradually increased and plotted against the efficiency. Fig. 8 shows the result of an efficiency measurement in ratio 0.64.

Fig. 8. shows that the efficiency improvement when using

the slip controller is quite significant, especially for low engine torques. Since the average engine torque in normal drive cycles is usually relatively low, this is a very promising result. For ratios until ratio 1.4, the efficiency improvement is a little lower than for low ratios, but still in the order of 10 to 5%. For higher ratios than 1.4, the efficiency improvement becomes less. When driving in overdrive, there is hardly any improvement. This is caused by the minimum pressure level in the CK2 of 0.66 MPa, which results in a minimum clamping force of almost 10 kN. Lower clamping forces are required for slip control in ratios near overdrive.

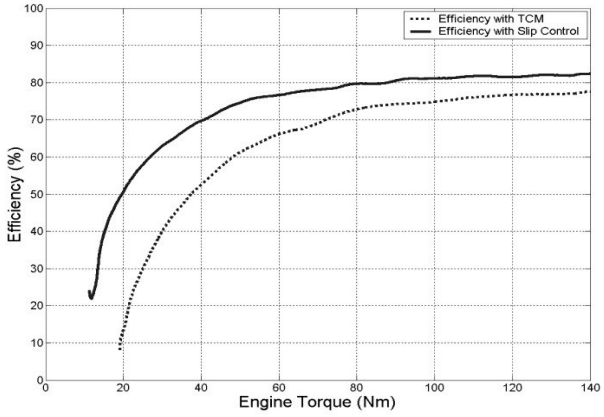

Fig. 8. Comparison of efficiencies between TCM and slip control, measured for ratio 0.64, at an engine speed of 300 rad/s.

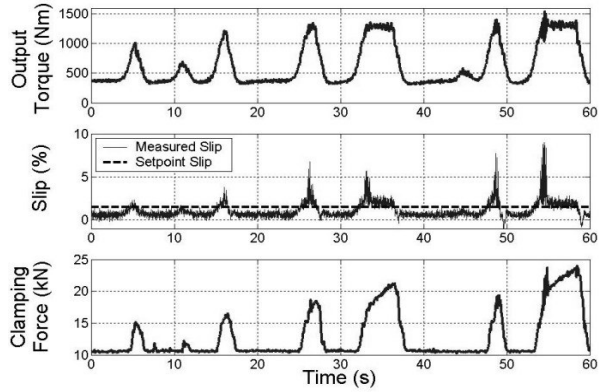

Fig. 9. Slip controller performance with torque peaks acting on the driveline, measured for ratio 0.43 (low), at an engine speed of 200 rad/s.

C. Load disturbance measurements

The previous section shows that slip control significantly increases the efficiency of a CVT. This was to be expected, based on previous studies. The next step is to perform experiments where torque peaks are introduced in the driveline, thus testing the performance of the slip controller with load disturbances. Also interesting in these tests are the amounts of slip that occur using slip control and whether this damages the belt and pulleys. Experiments were performed at fixed ratios and with a fixed engine speed of 200 rad/s. The slip was controlled at the same values that were used for the efficiency measurements. The eddy-current brake provided a constant torque high enough to reach a slip value at the transition between the micro- and macroslip region. Torque peaks were then introduced by suddenly engaging the disc brake. Fig. 9. Shows the result of one of these measurements.

The figure shows that the slip controller is able to deal with torque peaks of up to 1000 Nm in the drive shaft, although this causes the slip level to peak above 5% for short periods of time. Visual inspection however, showed that the belt was not damaged after such tests.

VI. Conclusion

The developed slip controller shows efficiency improvements of the Jatco CK2 of up to 30% at low engine torques. At higher engine torques and high ratio this gain is less.

Using the slip controller it is possible to operate a CVT with minimal clamping forces, while preventing damage to the belt and pulleys. Relatively high slip levels (5-15%), which were present for very short periods of time during the tests, did not lead to damage to the system. The slip controller is able to attenuate load disturbances of up to 1000 Nm in the driveshaft and perhaps even more. This is true for the current test conditions, but more research is necessary to investigate the long-term effect of using slip control in a wide range of working points with respect to belt damage.

The next step is to implement the slip controller in a car to explore the possibilities of slip control even further.

Acknowledgment

The authors thank Jatco Japan for providing us with test transmissions, spare parts, and support during the project.

References

[1] J. D. Micklem, D. K. Longmore and C. R. Burrows, “The magnitude of the losses in the steel pushing V-belt continuously variable transmission,” Proc Instn Mech Engrs Vol. 210, Part D: Journal of Automobile Engineering, ImechE, 1996

[2] B. Bonsen, T. W. G. L. Klaassen, K. G. O. van de Meerakker, M. Steinbuch and P. A. Veenhuizen, “Analysis of slip in a continuously variable transmission,” Proceedings of IMECE’03, ASME International Mechanical Engineering Congress, Washington, D.C., November 15-21, 2003

[3] M. van Drogen, M. van der Laan, “Determination of variator robustness under macroslip conditions for a push belt cvt,” SAE world congress 2004.

[4] Keiju Abo, Masayuki Kobayashi and Minoru Kurosawa, “Development of a Metal Belt-Drive CVT Incorporating a Torque Converter for Use with 2-Liter Class Engines,” SAE International Congress and Exposition, Detriot, Michigan, February 23-26, 1998

[5] H. Panagopoulos, K. J. Åström and T. Hägglund, “Design of PID controllers based on constrained optimization,” IEE Proc.-Control Theory Appl., Vol. 149, No. 1, January 2002

[6] B. Bonsen, T. W. G. L. Klaassen, K. G. O. van de Meerakker, P. A. Veenhuizen and M. Steinbuch, “Measurement and control of slip in a continuously variable transmission”, in Mechatronics 2004, Sydney, Australia, 2004